Ventilation, Potential-Vorticity Homogenization and the Structure of the Ocean Circulation[1]

J. PEDLOSKY

Woods Hole Oceanographic Institution, Woods Hole, MA 02543

W. R. YOUNG

Marine Physics Laboratory of the Scripps Institution of Oceanography, La Jolla, CA 92093

(Manuscript received and in final form 12 May 1983)

ABSTRACT

A model for the vertical structure of the oceanic circulation is presented that combines elements of the theory of the ventilated thermocline, given by Luyten, Pedlosky and Stommel, with the theory of Rhines and Young for the wind driven circulation of an unventilated ocean.

Our model consists of a ventilated thermocline region above an unventilated zone in which motion is limited to pools of constant potential vorticity. The model is nonlinear and hence the presence of ventilation affects the dynamics of the unventilated motion and vice-versa.

The planetary geostrophic equations are used and so the quasi-geostrophic assumption of Rhines and Young is relaxed, allowing large isopycnal excursions.

It is shown that the presence of ventilation generally shrinks and weakens the size and vigor of the subsurface pools of homogenized potential vorticity. At the same time, within those domains, the strength of circulation in the ventilated zone is somewhat diminished as the subsurface layers carry a portion of the Sverdrup transport.

We argue that the (mathematically) consistent circulation in the absence of sub-thermocline constant potential-vorticity pools is unstable.

The non-uniqueness of the nondissipative Sverdrup dynamics is demonstrated by the ambiguity in the specification of potential vorticity in the deeper, unventilated layers. The study emphasizes the subtle importance of dissipation in selecting a unique solution.

1. Introduction

Two theories have recently been advanced to explain the vertical and horizontal structure of the wind-driven oceanic circulation and the accompanying distribution of density.

The first theory (Rhines and Young, 1982a, hereafter RY); Young and Rhines, 1982) uses what we call an unventilated model of the ocean. In the layered version of this theory, only the uppermost layer is exposed to the surface and is forced by the wind stress. In the absence of dissipation (that is, no smaller scale processes such as mesoscale eddies), there are an infinite number of steady solutions for the resulting flow. In one possible solution all of the wind-driven flow is confined to the uppermost layer. However, if the wind forcing is strong enough, the isopleths of potential vorticity in the next lowest layer will become sufficiently distorted to overcome the β-effect and produce closed geostrophic contours. Geostrophic motion is then not prohibited by the no-flux eastern boundary condition. RY argue that this motion will, in fact, be induced by baroclinic instability associated with mesoscale eddies which redistribute the wind-driven flow vertically. The motion on the closed geostrophic contours, which coincide with the potential vorticity isopleths, is not determined uniquely in a dissipation-free model. Using an extension of the Prandtl–Batchelor theorem and the hypothesis that lateral diffusion of potential vorticity is the dominant dissipative mechanism (Rhines and Young, 1982b), it is argued that within the closed geostrophic contours, the potential vorticity becomes homogenized horizontally. As a result, the wind-driven flow penetrates downward layer-by-layer forming pools of constant potential vorticity within each deep layer. The subsurface motion is then limited to a bowl-shaped region in which the lateral extent diminishes with depth and the overall extent depends on the vigor of the wind forcing. Since the mesoscale eddy stresses are approximately proportional to the gradient of mean potential vorticity (Rhines and Holland, 1979), they vanish in the region of homogenized potential vorticity. This particular prediction is strikingly confirmed by Holland's (1983) numerical simulation of an unventilated ocean.

The unventilated model described in RY uses the standard β-plane quasi-geostrophic approximation.

[1] Woods Hole Oceanographic Institution Contribution No. 5415.

This allows only small overall departures of isopycnal depths (or layer thicknesses) from their resting values. A cursory inspection of an oceanographic atlas shows that this condition is not satisfied by planetary scale flows. In particular, when the forcing is strong enough to produce closed potential-vorticity contours, it will usually lead to significant excursions of isopycnal surfaces from their resting levels. Nor can the quasi-geostrophic theory describe the process in which isopycnal surfaces strongly deform and intersect the sea surface to expose deeper layers to wind forcing.

The second theory (Luyten *et al.*, 1983—hereafter LPS) uses a ventilated model of the ocean. The theory is closer in spirit to the classical thermocline theories (e.g., Needler, 1967; Welander, 1971) than is that of Rhines and Young. It abandons the β-plane approximation and allows large departures of isopycnal depths on planetary scales. It is able to satisfy vertical and horizontal boundary conditions in a more convincing fashion than the classical theories although this is only accomplished through the use of a layered model of the oceanic thermocline. The key feature of the ventilated model is the outcropping of isopycnal surfaces at the sea surface. Fluid at the surface is subducted beneath less dense fluid at more southerly latitudes, from which point the fluid conserves potential vorticity. The theory predicts the gross structure of the thermocline and the associated deep motion field as a direct consequence of the surface distribution of density and Ekman pumping. In this second model subsurface motion requires ventilation and subduction rather than homogenization of potential vorticity. The two theories predict different domains of subsurface motions.

An important assumption in LPS is that the layers beneath the ventilated thermocline are at rest. This an arbitrary choice. Although it is self-consistent, it is merely one of an infinite number of possible steady solutions. The nonuniqueness arises because LPS completely avoid consideration of dissipative processes. As in RY, a lack of uniqueness is present in the specification of flow in the unventilated region. If the layer beneath the deepest *ventilated* layer is thin enough (or equivalently if the forcing is strong enough), then potential vorticity contours in the resting, unventilated layer may close and, as in the first theory, a deep recirculating gyre of homogenized potential vorticity can be formed beneath a ventilated thermocline. Indeed, a limiting case occurs when the unventilated layers become so thin that, were they assumed to be motionless, the ventilated layers would slice through them from above forming strong lateral density discontinuities.

The purpose of this paper is to present a synthesis of the ideas of the two theories. The new hybrid theory incorporates desirable features of both the ventilated and unventilated models. It supersedes the theory of RY by including the effects of isopycnal outcrops, subduction and ventilation and it further avoids the quasi-geostrophic β-plane approximation. We believe it is superior to the LPS model because it explicitly considers the effect of eddy-induced mean flow acceleration around closed geostrophic contours in the unventilated regions beneath the ventilated layers.

It is important to note that the synthesis of the two models involves more than simply stacking the ventilated model atop an unventilated zone. At each horizontal location, the sum of the northward transports in the two regions must satisfy the Sverdrup relation. This condition links the ventilated and unventilated regions in a nonlinear fashion. This nonlinearity renders the required analysis more complicated, if not more difficult, than in earlier theories.

In common with the earlier theories, certain hypotheses must be made to avoid the underlying nonuniqueness of the nondissipative dynamics we consider. As in RY, we assume that dissipation by mesoscale eddies acts to homogenize the potential vorticity in unventilated regions whose bounding geostrophic contour is either closed or, if not closed in the oceanic interior, at least avoids intersecting the eastern boundary of the ocean. There is also an assumption about the western boundary layer dynamics: Ierley and Young (1983) show that homogenization does not occur if the boundary layer is diffusive. However, we wish to stress the important point which emerges unequivocally from the present study that the planetary geostrophic, ideal-fluid equations do not have a unique solution. Some dissipative process is required to select a solution and a different weak dissipative process will select a different solution. If one argues that a particular solution is more "realistic" than another one, one is asserting that a particular dissipative process is dominant in the ocean. In this article, as in RY, we hypothesize that the dominant dissipative process, due to mesoscale eddies, is lateral diffusion of potential vorticity.

Another very subtle role of dissipation and mixing is implicit in our use of finite layers for some aspects of the model. The use of a continuous, nondissipative model implies that fluid cannot cross a density surface no matter how slight is the density contrast with a neighboring density surface. The use of finite layers may actually better model the situation where the restraint against cross-isopycnal mixing only occurs for finite intervals of density change. An alternative suggestion is that very thin layers will be so strongly coupled by vertical stresses that their dynamics is equivalent to that of fewer, thicker layers (Ierley and Young, 1983).

In this paper, as in the earlier theories, the actual process of thermal forcing is not explicitly considered. Rather, this process is translated to a specification of the density distribution at the sea surface and along the ocean's eastern boundary (or equivalently, in our model, on the latitude of zero Ekman pumping). This specification is the implicit result of some deep nongeostrophic process, such as deep convection. Alternatively, some of the specification of the density field

required by our model may be the result of dynamic processes in the western boundary-current region which is beyond the scope of the present theory.

As in the earlier theories, the fundamental physics used is very simple. The motion is assumed to be completely geostrophic, hydrostatic and density conserving. At the sea surface an Ekman pumping velocity w_E is specified. It is negative in the subtropical gyre and positive in the sub-polar gyre and vanishes at the latitude where Coriolis parameter is f_0. Throughout, we assume that the geostrophic zonal velocity must vanish at the eastern wall, $x = a$.

In the following sections we present several simple models that describe the interplay between ventilation and potential vorticity homogenization. In Section 2 we describe a model in which the ventilated region consists of only one homogeneous layer which overlies a continuously stratified unventilated region. The buoyancy frequency is a linear function of depth in the unventilated zone. This model is the extreme limit of a unventilated domain with very thin (here infinitesimally so) isopycnal layers. The effect of Ekman pumping in the subtropical gyre is felt quite strongly in the unventilated zone. In fact, to preserve continuity of density deep motion is required. In Section 3 we use a layered model of both the unventilated and ventilated regions. This allows us to describe somewhat more general stratification of the unventilated zone and to determine the effect of outcropping and enhanced ventilation on the zones of constant potential vorticity. In Sections 2 and 3 we find that since pools of constant potential vorticity carry some of the required Sverdrup transport, they diminish the strength of flow in the ventilated region. Section 3 also demonstrates a further coupling, namely that the presence of ventilation and outcropping shrinks the size of the pools of constant potential vorticity.

Section 4 is a discussion of the flow in the sub-polar gyre using the model of Section 2, and it stresses the absence of unique solutions. We conclude in Section 5 with a discussion of our results.

2. Continuously stratified models of the subtropical gyre

a. *Equations of motion*

Throughout this article we use the planetary geostrophic equations (Phillips, 1963, or Pedlosky, 1979, Section 6.20). This approximation is appropriate when the Rossby number (U/f_0L in standard notation) is small and the horizontal length scale of the flow is comparable to the radius of the Earth (i.e., $\beta L/f_0 \leqslant 1$ but not $\ll 1$). The β-plane approximation is not made so that in the equations of motion, f is a function of the north–south coordinate y. Here β is defined by

$$\beta(y) \equiv \frac{df}{dy}, \tag{2.1}$$

and it is also convenient to use the notation

$$f_0 = f(0). \tag{2.2}$$

The coordinates (x, y, z) are Cartesian. Gill (1982) shows how to transform the equations of motion in spherical coordinates into the Cartesian system below. The vertical coordinate z is positive upwards and $z = 0$ is the base of the mixed layer. The velocity is (u, v, w), and the motion is forced by Ekman pumping or suction at the base of the mixed layer:

$$w(x, y, 0) = w_E(x, y). \tag{2.3}$$

The three components of the momentum equation are:

$$-fv = -\frac{p_x}{\rho_0}, \tag{2.4a}$$

$$fu = -\frac{p_y}{\rho_0}, \tag{2.4b}$$

$$0 = p_z + \rho g, \tag{2.4c}$$

where p is the pressure, g the gravitational acceleration, ρ the density and ρ_0 is the mean density of the fluid. The Boussinesq approximation is made so the fluid is incompressible:

$$u_x + v_y + w_z = 0. \tag{2.5}$$

It is convenient to represent the density as

$$\rho = \rho_0[1 - g^{-1}B],$$

where B is buoyancy.

By eliminating the pressure from (2.4) one obtains the three components of the vorticity equation

$$fv_z = B_x, \tag{2.6a}$$

$$fu_z = -B_y, \tag{2.6b}$$

$$\beta v = fw_z. \tag{2.6c}$$

Eqs. (2.6a,b) are the thermal-wind relations while (2.6c) is the Sverdrup balance connecting vortex stretching and north–south velocity.

A result we will use frequently is obtained by eliminating v between (2.6a) and (2.6c)

$$f^2w_{zz} = \beta B_x. \tag{2.7}$$

The final equation which closes the system is conservation of density

$$uB_x + vB_y + wB_z = 0. \tag{2.8}$$

Differentiating (2.8) with respect to z and using (2.6) gives conservation of potential vorticity:

$$uq_x + vq_y + wq_z = 0, \tag{2.9a}$$

$$q \equiv fB_z. \tag{2.9b}$$

Finally, in a layer model in which the density changes are localized at surfaces, (2.6a and b) are

$$f(\delta v) = (\delta B)h_x, \tag{2.10a}$$

$$f(\delta u) = -(\delta B)h_y, \tag{2.10b}$$

where $(\delta u, \delta v)$ is the jump in velocity at the surface, δB is the jump in buoyancy and $z = -h(x, y)$ is the position of the surface separating the two layers.

b. A ventilated model of the subtropical gyre

In this subsection we present a "ventilated" model of the wind driven circulation. The term ventilated refers to the assumption that only the density layers directly forced by the wind are in motion.

The underlying stratification is shown in Fig. 1. It consists of a layer of fluid with uniform density, $B = 0$, riding over a continuously stratified fluid. For simplicity, it will be assumed that the buoyancy of this unventilated region is

$$B = N^2(z + H_*). \tag{2.11}$$

At the eastern boundary, $x = a$, the stratification is undisturbed by the forcing (e.g., RY and LPS) and the layer of homogeneous fluid has uniform thickness H_0. Thus, at the eastern boundary there is a buoyancy jump,

$$\delta B = N^2(H_0 - H_*), \tag{2.12}$$

and static stability requires $H_0 > H_*$. Away from the eastern boundary the thickness of the upper layer will be denoted by $D(x, y)$ (see Fig. 1). The surface $z = -D(x, y)$ separates the ventilated fluid from the motionless unventilated fluid below.

The assumption (2.11), together with the assumption that there is only one surface density layer can be relaxed. In fact, one can, in principle, take the underlying stratification to be an arbitrary function of z and also, as in LPS, insert additional density layers that surface at prescribed latitudes in the subtropical gyre.

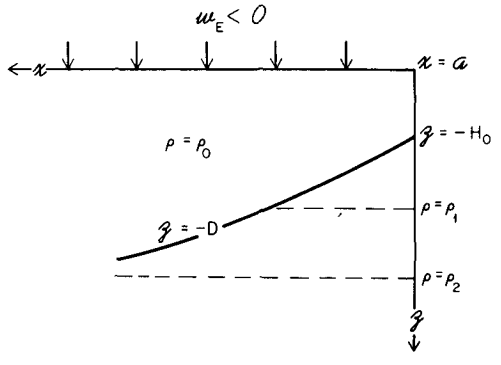

FIG. 1. A schematic zonal density section of the subtropical gyre. The stippled area above $z = -D(x, y)$ represents fluid of uniform density injected from the Ekman layer at $z = 0$. Below $z = -D(x, y)$ the fluid is stratified and the dashed lines represent undisturbed isopycnals. Note how the strength of the density jump at $z = -D$ increases with depth.

To solve the equations of motion, begin by observing that at $z = -D$ there is a buoyancy jump

$$\delta B = N^2(D - H_*). \tag{2.13}$$

Now from (2.6a,b) the velocities are independent of z in the ventilated region. Vertically integrating (2.6c) from $z = 0$, where $w = w_E$, to $z = -D$, where $w = 0$ (because the unventilated layers are motionless) gives

$$v = \frac{fw_E}{\beta D}. \tag{2.14}$$

At $z = D$, the density is discontinuous, and (2.10) and (2.13) give

$$fv = N^2(D - H_*)D_x. \tag{2.15}$$

Eliminating v using (2.14) gives a simple differential equation for D:

$$(D - H_*)DD_x = \frac{f^2 w_E}{N^2\beta}. \tag{2.16}$$

Integrating the above from $x' = x$ to $x' = a$ gives

$$\tfrac{1}{3}D^3 - \tfrac{1}{2}D^2H_* = -\left(\frac{f^2}{N^2\beta}\right)\int_x^a w_E dx' + \left(\tfrac{1}{3}H_0^3 - \tfrac{1}{2}H_0^2H_*\right). \tag{2.17}$$

Note how the above satisfies the boundary condition $D = H_0$ at $x = a$. It is straightforward to show that the cubic in (2.17) has one physically reasonable solution: the spurious solutions are rejected by recognizing that static stability requires $D > H_*$.

Once D has been calculated from (2.17) one has

$$w = w_E[1 + (z/D)] \tag{2.18}$$

and then from (2.6c):

$$v = \frac{fw_E}{\beta D} \tag{2.19a}$$

$$= \left(\frac{N^2}{f}\right)(D - H_*)D_x, \tag{2.19b}$$

$$u = -\left(\frac{N^2}{f}\right)(D - H_*)D_y. \tag{2.20}$$

c. Some comments on the density field

Perhaps the most unrealistic feature of the model described here is the intersection of the resting, flat isopycnals below $z = -D$ with the fluid injected from the mixed layer (see Fig. 2, 3, 4 and 5). It is important to realize that similar singularities would occur if the unventilated region were layered: LPS avoided this intersection by implicitly assuming that the uppermost unventilated layer was sufficiently thick. However, it is easy to see that in general the surface $z = -D$ would progressively slice through thinner, quiescent unventilated layers. The calculation in the preceding subsection exaggerates this effect (or perhaps represents it

accurately) by using a continuously stratified model of the unventilated region. One can think of the LPS solution and the present solution as endpoints of a continuum of models in which the vertical resolution of the unventilated region is increased by making the layers finer and finer.

d. Summary of the ventilated model

The calculation in the previous subsections is summarized in Figs. 2, 3, 4 and 5. In these figures the subtropical gyre is the region $y < 0$ where $w_E < 0$. The circulation patterns shown in the region $y > 0$ (i.e., the subpolar gyre where $w_E > 0$) are calculated using the theory of Section 4. Also, in all these figures it has been assumed that

$$H_* = H_0 = 0, \tag{2.21a}$$

$$\frac{d\beta}{dy} = 0. \tag{2.21b}$$

Figure 2 shows a meridional section. Here D has been calculated from (2.17) using (2.21) and

$$f^2 w_E = f_0^2 w_0 \left(\frac{\beta y}{f_0}\right). \tag{2.22}$$

Thus $y = 0$ is the boundary between the gyres and (2.22) is a local approximation to the forcing function at this latitude. Note that the stratification is undisturbed at $y = 0$.

Figure 3 shows a sequence of zonal sections through the gyres. Below the surface $z = -D$ the density field is undisturbed and is given by (2.11) with $H_* = 0$. Also at $y = 0$, where the Ekman pumping vanishes, the isopycnals are flat and the fluid is motionless.

In order to visualize the circulation in a complete double gyre system (refer to Section 4 for the theoretical discussion of the subpolar gyre) consider the forcing pattern

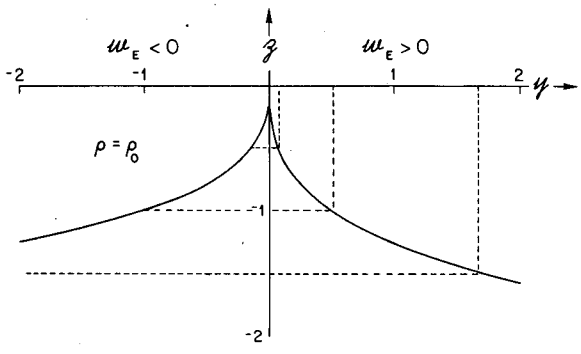

FIG. 2. A meridional section showing the density field (the dashed lines are isopycnals) in the vicinity of the latitude where $w_E = 0$. The surface $z = -D(x, y)$ is the solid curve. The section is at $x = 0$ and $w_E = 0$. The surface $z = -D(x, y)$ is the solid curve. The section is at $x = 0$ and w_E is given by (2.22). The north–south distance is nondimensionalized by some arbitrary length scale L and the depth is nondimensionalized by $(f_0 a L w_0/3N^2)^{1/3}$.

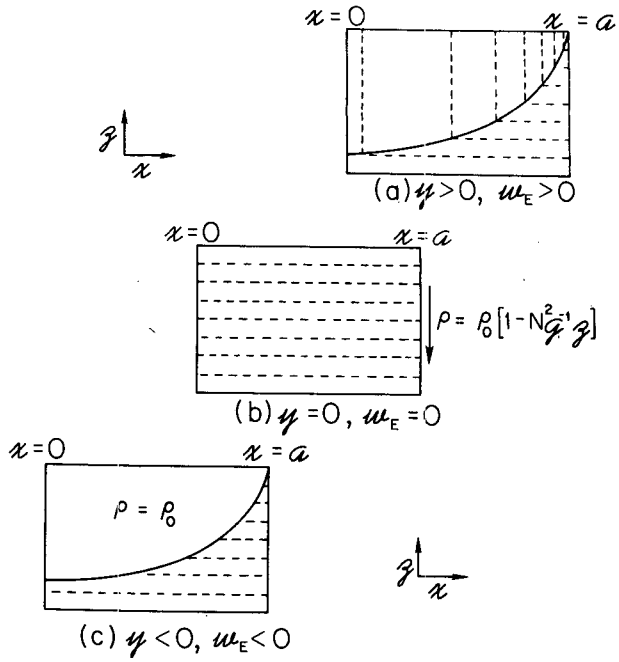

FIG. 3. A sequence of zonal sections through the gyre: (a) a zonal section in the subpolar gyre, (b) a zonal section at the boundary between the subpolar and subtropical gyres and (c) a zonal section in the subtropical gyre. The dashed curves are isopycnals while the solid curve is $z = -D$. It has been assumed that $\partial w_E/\partial x = 0$ so $D \propto (a - x)^{1/3}$ and $H_0 = 0$. In (b) the basic stratification is undisturbed since $D = 0$ at this latitude.

$$w_E = \left(\frac{f_0}{f}\right)^2 w_0 \sin\left(\frac{\pi y}{L}\right), \tag{2.23}$$

where $-L < y < L$. When $y < 0$, w_E is negative while when $y > 0$, w_E is positive. Thus (2.23) models the Ekman pumping in a double gyre system where once again $y = 0$ is the boundary between the gyres. In Fig. 4 contours of constant pressure are plotted at two depths: $z = 0$ and $z = \frac{1}{2}D_{\max}$, where

$$D_{\max}^3 = \frac{6 f_0^2 w_0 a}{N^2 \beta}$$

is the maximum depth of the gyre. These pressure contours are "streamlines" for the nondivergent vector field (fu, fv). Fig. 5 shows a meridional density section through the double gyre system.

Perhaps the most peculiar feature of the ventilated model is the way in which the isopycnals intersect. It is likely that although these are exact solutions of the planetary geostrophic equations, other processes must intervene and prevent the flow in Figs. 2–5 from becoming established. The process favored by RY is vertical stress transmission produced by mesoscale eddies. A variety of simple arguments suggest that this mechanism may produce large mean flows when there are closed geostrophic contours, i.e., unimpeded free flow paths. Now it is apparent from Fig. 2 that the geostrophic contours in the motionless, stratified fluid im-

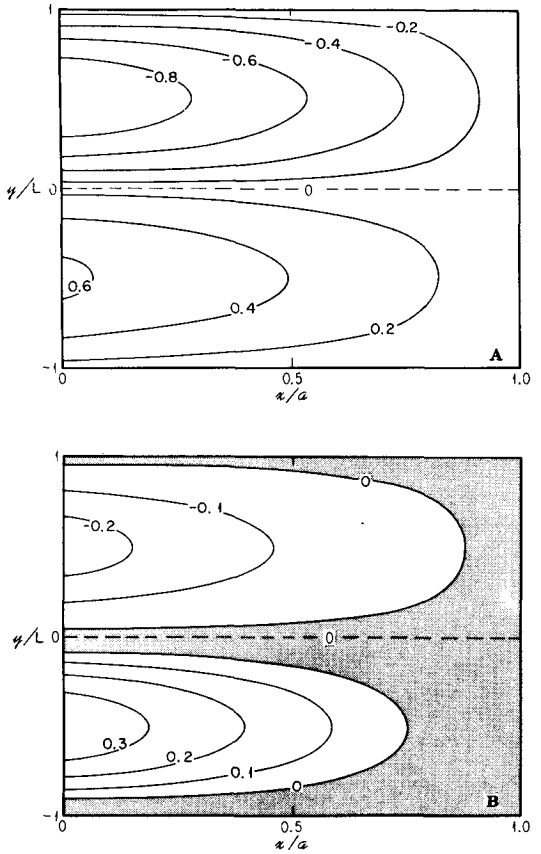

FIG. 4. A plan view of the pressure field [actually $(p/\rho_0 = gz = \frac{1}{2}N^2z^2)/(\frac{1}{2}N^2D^2_{max})$] in a double gyre system at two depths, (a) $z = 0$ and (b) $z = \frac{1}{2}D_{max}$.

mediately below $z = -D$ track the base of the gyre. Thus the region immediately below $z = -D$ in Fig. 2 is particularly susceptible to mean flow acceleration. This argument suggests a model where there is a region of ventilated fluid with density ρ_0, injected from the mixed layer, riding above a region where eddy stresses have removed all the closed geostrophic contours by homogenizing the potential vorticity. This alternative leads to the model developed in the next subsection.

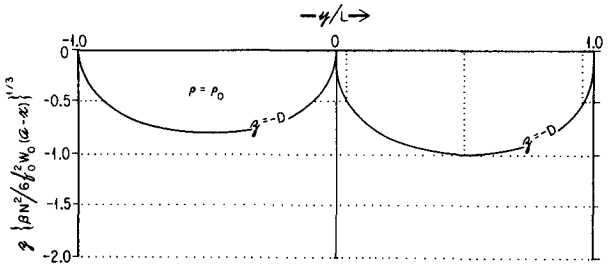

FIG. 5. A meridional density section through the double gyre system. The solid curve is $z = -D(x, y)$ while the dashed curves are isopycnals.

e. A partially ventilated model of the subtropical gyre

In this section we present a partially ventilated model of the wind-driven circulation. The designation of partial ventilation refers to the assumption that the density layers below those directly forced by the wind are also in motion. This notion allows one to construct a circulation which does not have some of the singularities found in the earlier section (e.g., intersecting isopycnals).

As in the previous section, fluid of density ρ_0 is pumped out of the Ekman layer. This fluid collects above a region where the potential vorticity is uniform (see Fig. 6). As in RY, the value of the constant potential vorticity in this region is determined by conditions at the boundary between the subtropical and subpolar gyre. As in the previous subsections, this boundary is at $y = 0$ where $f = f_0$. Below the region of uniform potential vorticity lies motionless fluid in which the stratification is given by (2.11).

Thus the ocean is divided into three regions (Fig. 6):

1) Region I where $0 > z > -D(x, y)$ and $\rho = \rho_0$ or equivalently $B = 0$.

2) Region II where $-D(x, y) > z > -G(x, y)$ and $q = fB_z = f_0N^2$. The potential vorticity is uniform on isopycnals and because of the special assumption (2.11) uniform across isopycnals.

3) Region III where $-G(x, y) > z > -\infty$ and $B = N^2(z + H_*)$ as in (2.11) while $(u, v, w) = (0, 0, 0)$.

We have assumed that the basic stratification is given by (2.11). In general the functional relationship between q and ρ in Region II is obtained by eliminating z between B and fB_z at the northernmost point of the subtropical gyre (RY). Young and Rhines (1982) discuss a case where the stratification is exponential with depth. At this point the fluid is motionless at all depths

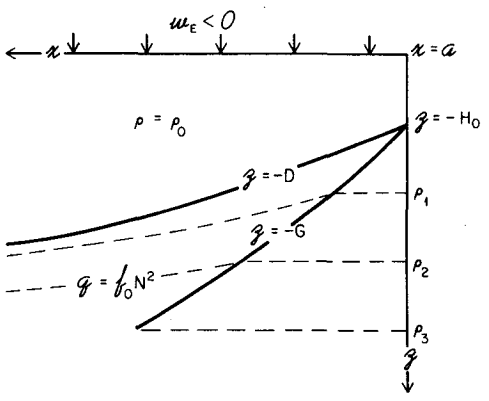

FIG. 6. A schematic zonal density section of the subtropical gyre. The dashed curves represent isopycnals. Above $z = -D$ lies the fluid with density ρ_0 injected from the mixed layer. Between $z = -D$ and $z = -G$, the potential vorticity is uniform. Below $z = -G$, the fluid is motionless. At $x = a$, the stratification is undisturbed.

and the basic stratification is undisturbed. It seems likely that one could construct a family of solutions by assuming different functional relations between q and B in Region II. The choice of uniform q is motivated by the Prandtl–Batchelor theorem discussed by Rhines and Young (1982b).

In Region II where $q = fB_z = f_0N^2$, it follows that

$$B = \left(\frac{f_0N^2}{f}\right)z + b(x, y), \quad -D > z > -G. \quad (2.24)$$

One can now obtain two relations between the three unknowns G, D and b by matching the density field at $z = -D$ and $z = -G$.

At $z = -D$ we require that the same buoyancy jump occurs at the base of the ventilated region as occurs at the eastern boundary. Thus

$$-\left[-\left(\frac{f_0}{f}\right)N^2D + b\right] = N^2(H_0 - H_*)$$

or

$$b = \left(\frac{f_0}{f}\right)N^2D - N^2(H_0 - H_*) \quad (2.25)$$

so that when $-D > z > -G$,

$$B = \left(\frac{f_0}{f}\right)N^2(z + D) - N^2(H_0 - H_*). \quad (2.26)$$

At $z = -G$ we require that the density be continuous. Thus putting $z = -G$ in (2.26) and (2.11) and equating the two, one has

$$D = G\left[1 - \left(\frac{f}{f_0}\right)\right] + \left(\frac{f}{f_0}\right)H_0. \quad (2.27)$$

Now if we can calculate G, we have a complete solution. To do this substitute (2.26) into (2.7) and integrate vertically upwards from $z = -G$. In order to make the transition to the motionless region below $z = -G$ as smooth as possible we choose the constants of integration so that v and w vanish at $z = -G$. One finds

$$v = \left(\frac{N^2}{f}\right)\left(\frac{f_0}{f}\right)\left[1 - \left(\frac{f}{f_0}\right)\right](z + G)G_x, \quad (2.28a)$$

$$w = \frac{1}{2}\left(\frac{\beta N^2}{f^2}\right)\left(\frac{f_0}{f}\right)\left[1 - \left(\frac{f}{f_0}\right)\right](z + G)^2G_x. \quad (2.28b)$$

Let $\hat{v}$ and $\hat{w}$ denote the values of v and w at $z = -D$. In Region I, the fluid has uniform density so $v = \hat{v}$ throughout the region and (2.6c) is

$$\beta\hat{v}D = f(w_E - \hat{w}). \quad (2.29)$$

At $z = -D$ there is a jump in buoyancy so (2.10a) is

$$f[\hat{v} - v(z = -D)] = \delta BD_x,$$

where v at $z = -D$ is evaluated from (2.28a). The $\hat{w}$ is determined by noting that w is continuous, so

$$\hat{w} = w(z = -D).$$

Using the above relations, one can eliminate $\hat{v}$, $\hat{w}$ and D from (2.29) and obtain an equation which determines G

$$\frac{1}{3}A(G - H_0)^3 + \frac{1}{2}B(G - H_0)^2 + C(G - H_0) = -\int_x^a w_E(x', y)dx', \quad (2.30)$$

where

$$\left.\begin{aligned} A &\equiv \left(\frac{\beta N^2}{f^2}\right)\left[1 - \left(\frac{f}{f_0}\right)\right]\left[1 - \left(\frac{f}{2f_0}\right)\right] \\ B &\equiv \left(\frac{\beta N^2}{f^2}\right)\left[1 - \left(\frac{f}{f_0}\right)\right] \\ &\quad \times \left\{H_0 + \left[1 - \left(\frac{f}{f_0}\right)\right](H_0 - H_*)\right\} \\ C &\equiv \left(\frac{\beta N^2}{f^2}\right)\left[1 - \left(\frac{f}{f_0}\right)\right](H_0 - H_*) \end{aligned}\right\}.$$

Because A, B and C are positive (provided f decreases as one moves south) it is easy to show that the cubic in (2.30) has one physically sensible solution, i.e., one solution for which $G > H_0$.

f. Local analysis of (2.30) near $y = 0$

It is informative to analyze (2.30) near $y = 0$. This is the boundary between the subpolar and subtropical gyres. Suppose further, as in Figs. 2–5, that

$$\left.\begin{aligned} H_* &= H_0 = 0 \\ \frac{d\beta}{dy} &= 0 \end{aligned}\right\}. \quad (2.31)$$

Because of (2.31), B and C vanish, and

$$A \approx -\frac{1}{2}\left(\frac{\beta N^2}{f_0}\right)^2\left(\frac{\beta y}{f_0}\right).$$

If in addition we employ (2.22) as a local approximation to w_E then (2.30) gives

$$G^3 = 6\left(\frac{f_0^2}{\beta N^2}\right)w_0(a - x). \quad (2.32)$$

Thus, in this second partially ventilated model of the wind-driven circulation, the depth of the circulation is not zero at the northern boundary when $H_0 = 0$. This is also apparent in the meridional density section shown in Fig. 7. The dotted curve in Fig. 7 indicates the depth of the circulation ($z = -D$) according to the earlier model. This figure should be compared with Fig. 2. The two theories predict very different flow patterns at the boundary between the two gyres. In the earlier theory, the depth of the gyre goes to zero (if $H_0 = 0$) as $y \to 0$, whereas in the present theory the circulation is deepest at the northern boundary. A

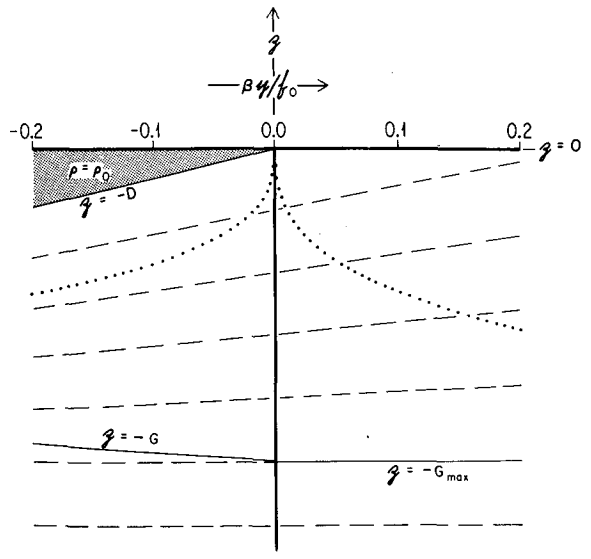

FIG. 7. A meridional section ($x = 0$) through the density field in the neighborhood of the boundary between the subtropical and subpolar gyres. The isopycnals are dashed. The boundaries $z = -D$ and $z = -G$ are solid. For comparison $z = -D$ from (2.17) and (2.22) is shown as a dotted curve.

deep northern boundary is more consistent with traditional descriptive ideas (e.g., Montgomery, 1938).

Note that the above remarks depend to some extent on the choice (2.31). To emphasize this point, consider the case

$$H_0 = H_* \neq 0. \tag{2.33}$$

In the neighborhood of $y = 0$, one can approximate (2.29) by

$$\tfrac{1}{3}\zeta^3 + \zeta^2 = E, \tag{2.34a}$$

$$E \equiv \frac{2f_0^2 w_0 (a - x)}{\beta N^2 H_0^3}, \tag{2.34b}$$

$$\zeta \equiv \frac{(G - H_0)}{H_0}, \tag{2.34c}$$

where once again (2.22) is used as a local approximation to w_E at $y = 0$.

Now if E is small, as it must be in the vicinity of the eastern boundary, then the approximate solution of (2.34a) is

$$\zeta \approx E^{1/2}, \tag{2.35}$$

or $G - H_0$ is proportional to $(a - x)^{1/2}$. This is qualitatively different from the solution when $H_0 = 0$: see (2.32).

When E is large, the approximate solution of (2.34) is

$$\zeta \approx (3E)^{1/3}. \tag{2.36}$$

The transition between the two limits (2.35) and (2.36) occurs when $E = O(1)$. If $w_0 = 10^{-4}$ cm s^{-1}, $(N/f_0) = 900$, $\beta = 1.6 \times 10^{-13}$ cm^{-1} s^{-1} and $H_0 = 800$ m (as in LPS), then E is of order 1 when

$$a - x \approx \beta\left(\frac{N}{f}\right)^2 \frac{H_0^3}{2w_0} \approx 3700 \text{ km}.$$

This distance is so large that the transition would probably not occur. However, the distance is very sensitive to the value of H_0. In the estimate above, H_0 was 800 m so that a large fraction of the thermocline is modeled by a single layer. If H_0 is reduced to 400 m, then the transition occurs at 460 km, and (2.32) is accurate over most of the basin.

g. Summary

The results of the calculation in this section are summarized in Figs. 8, 9 and 10. In these figures the circulation sketched in the subpolar gyre has been calculated using the theory of Section 4. Also, as in the earlier figures

$$H_0 = H_* = 0,$$

and (2.23) has been used as a model of Ekman pumping.

Two zonal density sections, one in the subpolar and the other in the subtropical gyre, are shown in Fig. 8. Because $D, G \to 0$ as $x \to a$, the stratification is undisturbed everywhere along the eastern boundary. Fig. 9 shows a meridional section through the double gyre system. Note how the isopycnal spacing increases pole-

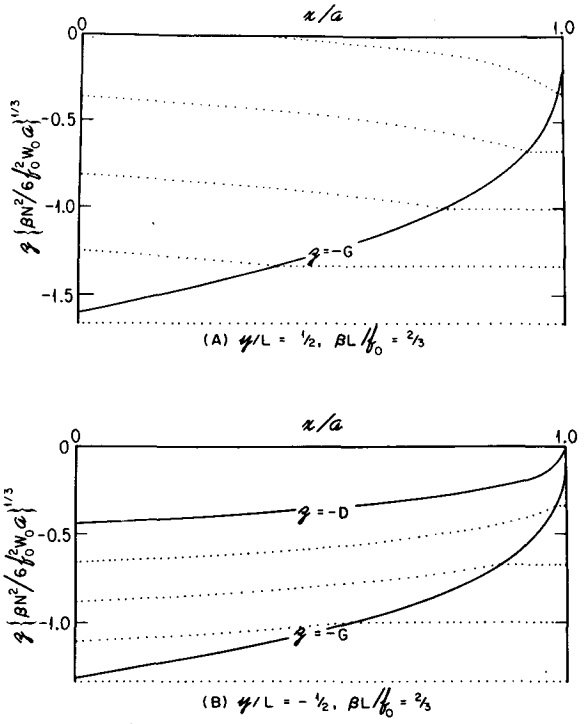

FIG. 8. Two zonal density sections in a double gyre system where w_E is given by (2.23): (a) a zonal section, through the subpolar gyre and (b) A zonal section through the subtropical gyre. The dotted curves are isopycnals. The surface $z = -g(x, y)$ is the solid curve. In (b) the solid curves are $z = -D(x, y)$ and $z = -G(x, y)$.

ward to ensure that the potential vorticity is uniform. Fig. 10 shows plan views of the pressure and density fields at two depths in the double gyre system. Fig. 10a is for $z = 0$ while Fig. 12b is for $z = -\frac{1}{2}G(0, 0)$. The stippled region in Fig. 10b has uniform density and is motionless. Many of the qualitative features of the circulation patterns above are already present in the simpler quasi-geostrophic model of Young and Rhines (1982).

3. Layered model of the subtropical gyre

In this section we consider the circulation in the subtropical gyre where the Ekman pumping w_E is negative and represent the circulation by the layered model shown in Fig. 11. In the model there are only two layers, with thicknesses h_0 and h_v, which are exposed to the surface, although it is straightforward to add more ventilated layers. The layer with thickness h_v exists only south of the outcrop latitude where f is equal to f_v. The Ekman pumping vanishes at $f = f_0 > f_v$. Below these two ventilated layers there are an arbitrarily large number of layers. We insist only that at least the very *deepest* of these layers be at rest. At the latitude where w_E vanishes, the layer thicknesses are constant and given by

$$h_n = H_n, \quad n = 0, 1, 2 \cdots N. \tag{3.1}$$

The density of each layer is constant and given respectively by $\rho_v, \rho_0, \rho_1 \cdots \rho_n \cdots \rho_N$.

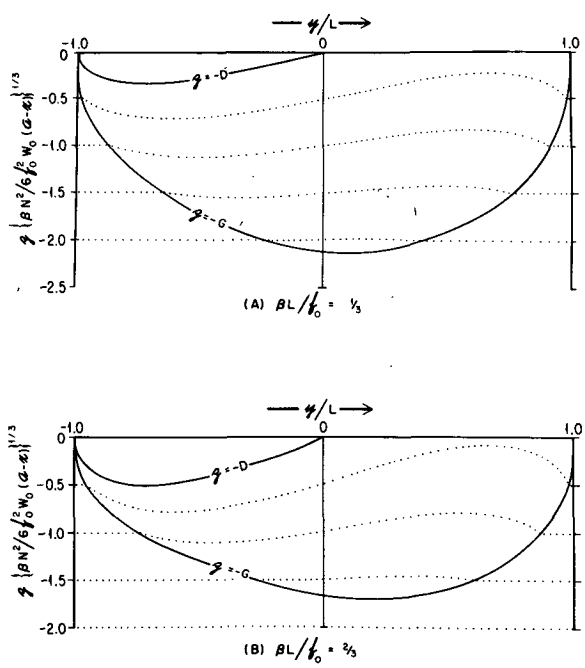

FIG. 9. Meridional density sections in a double gyre system: (a) $\beta L/f_0 = \frac{1}{3}$ and (b) $\beta L/f_0$ (c.f. Fig. 5). The dotted curves are isopycnals.

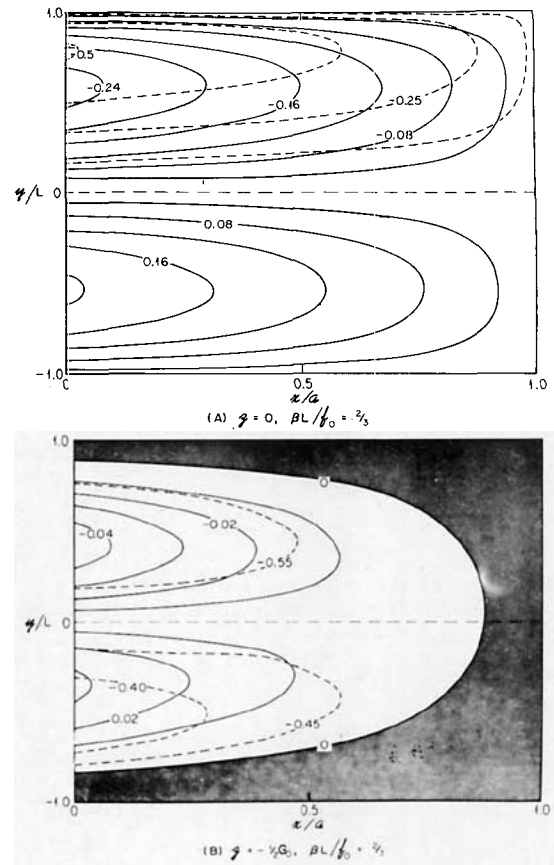

FIG. 10. Plan views of the pressure field [actually $(p/\rho + gz - \frac{1}{2}N^2z^2)/(\frac{1}{2}N^2G_0^2)$] and the density field (actually B/N^2G_0) at two depths in a double gyre system: (a) $z = 0$ and (b) $z = -\frac{1}{2}G(0.0) = G_0$. The isopycnals are dashed while the isobars are solid. In (a) the fluid in the subtropical gyre has uniform density at this depth. Note the change in the contour interval between (a) and (b). The shaded region represents motionless fluid.

Consider the case where n unventilated layers are in motion. Aside from an irrelevant term dependent only on depth, the pressure in each layer is given by

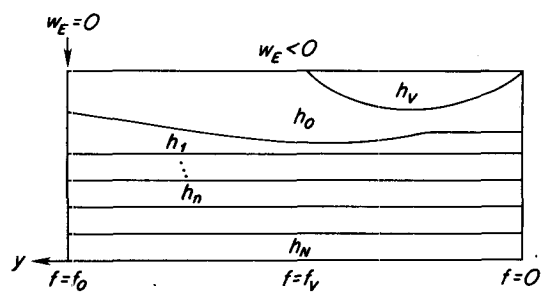

FIG. 11. A schematic meridional cross section of the layer model of the subtropical gyre. The layers with thicknesses h_0 and h_v are ventilated. The latter outcrops on the latitude where $f = f_v$. The Ekman pumping vanishes at $f = f_0$.

$$\left.\begin{aligned}
\frac{p_n}{\rho_n} &= \gamma_n(h_v + h_0 + \cdots h_n)\\
\frac{p_n}{\rho_n} &= \gamma_n(h_v + h_0 + \cdots h_n)\\
&\quad + \gamma_{n-1}(h_v + h_0 + \cdots h_{n-1})\\
&\vdots\\
\frac{p_1}{\rho_1} &= \gamma_n(h_v + h_0 + \cdots h_n)\\
&\quad + \gamma_{n-1}(h_v + h_0 + \cdots h_{n-1})\\
&\quad + \cdots \gamma_1(h_v + h_0 + h_1)\\
p_0 &= p_1 + \gamma_0(h_0 + h_v)\\
p_v &= p_0 + \gamma_v h_v
\end{aligned}\right\}, \tag{3.2}$$

where

$$\left.\begin{aligned}
\gamma_n &= \frac{\rho_{n+1} - \rho_n}{\rho_0} g, \quad n = 0, 1, \cdots\\
\gamma_v &= \frac{\rho_v - \rho_0}{\rho_0} g
\end{aligned}\right\} \tag{3.3}$$

and the Boussinesq approximation, $\rho_{j+1} - \rho_j \ll \rho_0$, has been used.

In each layer, the meridional and zonal velocities are geostrophic, i.e.,

$$fv_n = \frac{\partial}{\partial x}\frac{p_n}{\rho_n}, \quad fu_n = -\frac{\partial}{\partial y}\frac{p_n}{\rho_n}. \tag{3.4}$$

The Sverdrup relation relates the total meridional transport to the surface Ekman pumping. In a region where n unventilated layers are in motion

$$\beta[\sum_{j=0}^{n} v_n h_n + v_v h_v] = f w_E. \tag{3.5}$$

The geostrophic equation for v and the relation between the pressure and layer thicknesses allows (3.5) to be rewritten as

$$\frac{\partial}{\partial x}\{\gamma_n[h_v + h_0 + h_1 + \cdots h_n]^2 + \gamma_{n-1}[h_v + h_0 + \cdots h_{n-1}]^2 + \cdots \gamma_0[h_0 + h_v]^2 + \gamma_v h_v^2\} = 2\frac{f^2}{\beta} w_E. \tag{3.6}$$

If only $j < n$ unventilated layers are in motion, (3.6) still applies since, in that case

$$h_v + h_0 + h_1 + \cdots h_k, \quad j < k \leqslant n,$$

will be constant and equal to its value on the eastern boundary. Thus (3.6) may be immediately integrated to yield

$$\gamma_v h_v^2 + \gamma_0(h_v + h_0)^2 + \gamma_1(h_v + h_0 + h_1)^2 + \cdots \gamma_n(h_v + h_0 + h_1 + \cdots h_n)^2 = \gamma_0(D_0^2 + C_n), \tag{3.7}$$

where

$$\gamma_0 C_n = +\gamma_0 H_0^2 + \cdots \gamma_n(H_0 + H_1 + \cdots H_n)^2, \tag{3.8a}$$

$$D_0^2(x, y) = -\frac{2f^2}{\gamma_0 \beta}\int_x^a w_E(x', y)dx'. \tag{3.8b}$$

In (3.8a) we have anticipated the result that the depth of the outcropped ventilated layer h_v must vanish on the eastern boundary (LPS).

The basic hypothesis in our theory is that whenever an unventilated layer is in motion, it must have uniform potential vorticity. Thus when the kth unventilated layer is in motion

$$\frac{f}{h_k} = \text{constant}.$$

At the latitude where w_E vanishes, h_k is presumed known, i.e., $h_k = H_K$ there, thus

$$\frac{f}{h_k} = \frac{f_0}{H_K}, \tag{3.9}$$

$$h_k = \frac{f}{f_0} H_K, \quad 1 \leqslant k \leqslant n. \tag{3.10}$$

It is important to point out that our theory presumes that at $f = f_0$, the density–depth relation (γ_k, H_k) is known. Some process in addition to geostrophy must set this arbitrarily given density distribution. Our theory simply describes the way the distribution is altered within the gyre.

Since H_k and γ_k are arbitrary the density–depth distribution our layered model can represent is fairly general. Of course, the limitation to a layered rather than a continuous model is at first sight a drawback. However, given the existence of oceanic regions of low static stability, so-called pycnostads, the layer model may have its own claim to realism not shared by the continuous model with *constant* buoyancy frequency. We prefer to think of both models as accessible, tractable, limiting endpoints of the natural system, each of which reflects important aspects of the general problem.

Since the thicknesses of the unventilated layers are known, (3.7) becomes a single equation for the two unknowns, h_0 and h_v. As in LPS, this problem may be solved by first considering the region north of $f = f_v$ where h_v is zero and then using potential vorticity conservation to relate h_0 to h_v when the h_0 layer subducts beneath the uppermost warm water layer.

Consider the region

$$f_0 \geqslant f \geqslant f_v$$

in which h_v vanishes: then (3.7) may be solved for h_0. The solution for h_0 and (3.10) completely determines the flow where n layers are in motion. A little thought reveals, however, that the resulting solution cannot be

valid for all x. Each p_n must be independent of latitude at $x = a$ to avoid zonal flow into the eastern wall and from (3.2) this implies that each layer must have constant thickness at the eastern boundary. This condition is clearly violated by (3.10). Clearly, fluid cannot move southward along the eastern boundary and simultaneously have constant thickness and constant potential vorticity. Thus in some region $x_1 < x < a$ only the uppermost layer can be in motion. In that region $h_k = H_k$ for all $k \geq 2$ while from 3.7

$$h_0 = (D_0^2 + H_0^2)^{1/2}, \quad x_1(y) \leq x \leq a, \tag{3.11}$$

as in LPS and Young and Rhines (1982)[2].

The thickness of the unventilated layer beneath the uppermost layer is

$$\begin{aligned} h_1 &= H_1 + H_0 - h_0 \\ &= H_1 + H_0 - (D_0^2 + H_0^2)^{1/2} \end{aligned} \tag{3.12}$$

while all h_k, $k > 1$, are constant. Only the uppermost layer is moving. In principle, (3.11) and (3.12) are possible solutions for all $0 \leq x \leq a$. This, in fact, is the solution given in LPS. However, since D_0^2 is an increasing function of $(a - x)$, as long as $w_E < 0$, at some distance from the eastern boundary h_1 will vanish when D_0^2 satisfies

$$D_0^2(x_c, y) = 2H_1H_0 + H_1^2, \tag{3.13}$$

and the thinner the unventilated layer, the closer to the eastern wall this will occur. Vanishing layer thickness is equivalent to the intersecting isopycnals in the earlier model, e.g., Figs. 2 and 3. Of course, if H_1 is large enough, h_1 will remain positive and (3.11) and (3.12) are then acceptable solutions. However, east of the line, $x_c(f)$, where h_1 would vanish, the potential vorticity isopleths in Layer 1 become so distorted that they intersect the western rather than the eastern boundary. Along that critical curve, $x_1(f)$,

$$\frac{f}{h_1} = \frac{f_0}{H_1}, \tag{3.14}$$

and west of the curve the uppermost unventilated layer may move with constant potential vorticity (our choice). The value of that constant potential vorticity we specify is the value it assumes on the bounding contour, f_0/H_1, in order to maintain continuity of q, as in RY. Note that regardless of how small H_1 is chosen to be, our assumption that the unventilated layer is in motion will avoid vanishing layer thicknesses and intersecting isopycnals. To find that boundary, $x_1(f)$, we need only insist that h_1 and h_0 be continuous along $x_1(f)$. Thus,

$$h_1 = H_1 \frac{f}{f_0} = H_1 + H_0 - h_0 \tag{3.15}$$

from (3.12) and (3.14). Thus, along $x_1(f)$

$$h_0 = H_0 + H_1(1 - f/f_0), \tag{3.16}$$

while continuity of h_0 implies that (3.11) must be identical to (3.16) or that $x_1(f)$ is given implicitly by

$$\begin{aligned} &D_0^2(x_1(f), y) \\ &\quad = 2H_0H_1\left(1 - \frac{f}{f_0}\right) + H_1^2\left(1 - \frac{f}{f_0}\right)^2. \end{aligned} \tag{3.17}$$

Note that (3.17) implies that this contour always occurs *east* of the point where h_1 would vanish if the lower layer were motionless. The reader is also asked to verify that only the *first* unventilated layer can be moving in the region just west of $x_1(f)$.

Consider the case where w_E is a function only of latitude, or equivalently, only of f. Then

$$D_0^2 = -(a - x)\frac{2f^2}{\beta\gamma_0} w_E(f). \tag{3.18}$$

Therefore, the contour separating the regions of one and two moving layers is given by

$$\begin{aligned} [a - x_1(f)] = -\frac{\beta}{2f^2}\Bigg[&2H_0H_1\left(1 - \frac{f}{f_0}\right) \\ &+ H_1^2\left(1 - \frac{f}{f_0}\right)^2\Bigg] \Bigg/ w_E(f). \end{aligned} \tag{3.19}$$

As f approaches f_0, both numerator and denominator of (3.19) vanish. Using L'Hôpital's rule, the intersection of $x_1(f)$ with the northern boundary of the subtropical gyre occurs at

$$\begin{aligned} a - x_1(f_0) &= \gamma_0 \frac{\beta_0}{f_0^3} H_0H_1 \Bigg/ \frac{\partial w_E}{\partial f}(f_0) \\ &= \gamma_0 \frac{\beta_0^2}{f_0^3} H_0H_1 \Bigg/ \frac{\partial w_E}{\partial y}(f_0). \end{aligned} \tag{3.20}$$

A schematic sketch of $x_1(y)$ is shown in Fig. 12. The contour $x_1(f)$ lies generally on a line that moves southwestward from $f = f_0$. At $f = f_0$, the continuation of the isopleth of constant potential vorticity is the portion of the latitude circle between the intersection $x_1(f_0)$ and the western boundary. If the magnitude of w_E increases rapidly enough south of $f = f_0$, the curve may bend southeastward first but will eventually bend westward and intersect the $x = 0$ meridian wherever

$$\begin{aligned} D_0^2(0, f) &= -\frac{af^2}{\beta\gamma_0} w_E(f) \\ &= 2H_0\left(1 - \frac{f}{f_0}\right) + H_1^2\left(1 - \frac{f}{f_0}\right)^2. \end{aligned}$$

[2] More precisely they find in the quasi-geostrophic theory

$$h_0 = H_0 + \tfrac{1}{2}D_0^2/H_0$$

which is the weak forcing limit of (3.11).

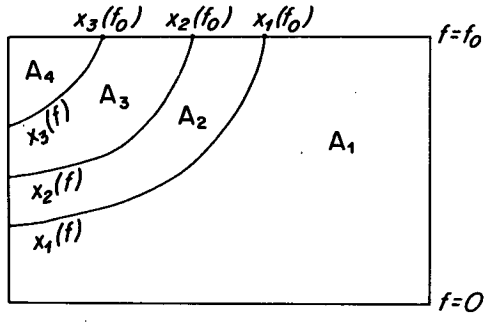

FIG. 12. The domains A_n of flow when there is one ventilated layer. East of $x_1(f)$, only the uppermost layer is in motion. In the regions $x_n(f) < x < x_{n-1}(f)$, $n-1$ *unventilated* layers are also moving with constant potential vorticity. The domains are nested about the northwest corner of the gyre where the deepest pools of constant potential vorticity are found.

If $w_E(0)$ is finite, this interaction must occur for a value of $f > 0$, i.e., the sector bounded by $x_1(f)$ must exclude the low-latitude ocean.

In the region just west of $x_1(f)$, there are two moving layers. The thickness of the motionless, second unventilated layer will then be a function of the motion above it. By a repetition of the previous argument, the thickness of this layer may sufficiently alter so that its potential vorticity isolines thread back to the western boundary layer. This will occur on the curve $x_2(f) < x_1(f)$—and so on. An obvious repetition of this argument, along with our hypothesis of potential-vorticity homogenization yields a nested series of curves $x_n(f)$ east of which there are n moving layers and west of which there are $n+1$ moving layers; n of them at constant potential vorticity. On $x_n(f)$, by a simple extension of the argument leading to (3.16)

$$h_0(x_n) = H_0 + (H_1 + H_2 \cdots H_n)(1 - f/f_0) \quad (3.21)$$

which with (3.7) yields the general equation for the extent of the constant potential-vorticity pool in the nth unventilated layer,

$$\begin{aligned} D_0^2(x_n) = {} & 2\gamma_0 H_0(H_1 + \cdots H_n)\left(1 - \frac{f}{f_0}\right) \\ & + \gamma_0(H_1 + H_2 + \cdots H_n)^2\left(1 - \frac{f}{f_0}\right)^2 \\ & + 2\gamma_1(H_0 + H_1)(H_2 + \cdots + H_n)\left(1 - \frac{f}{f_0}\right) \\ & + \gamma_1(H_2 + \cdots + H_n)^2\left(1 - \frac{f}{f_0}\right)^2 + \cdots \\ & + 2\gamma_{n-1}(H_0 + \cdots + H_{n-1})H_n\left(1 - \frac{f}{f_0}\right) \\ & + \gamma_{n-1}H_n^2\left(1 - \frac{f}{f_0}\right)^2 \quad (3.22) \end{aligned}$$

of which (3.17) is the special case, $n = 1$.

Once the domain of the constant potential-vorticity pool in each layer has been determined, (3.7) and (3.9) determine the layer thickness and therefore the motion. As in RY, the pools shrink with depth and slope northwestward. Of course, the solution for $x_n(f)$ given by (3.22) may lie entirely outside the ocean, i.e., for $x_n(f) < 0$, so that, in general, only a finite number of unventilated layers will be moving.

Consider the simplest case where only $x_1(f)$ lies in the interval $0 \leq x_n \leq 1$. In the region to the west of the $x_1(f)$, (3.7) yields

$$\begin{aligned} h_0(x, y) = {} & -\frac{\gamma_1}{\gamma_0 + \gamma_1} h_1 + \frac{1}{\gamma_0 + \gamma_1}[(\gamma_0 + \gamma_1) \\ & \times \{\gamma_0 D_0^2 + \gamma_0 H_0^2 + \gamma_1(H_1 + H_0)^2\} \\ & - \gamma_0\gamma_1 h_1^2]^{1/2}, \quad (3.23) \end{aligned}$$

where

$$h_1 = H_1 \frac{f}{f_0}$$

while east of $x_1(f)$, h_0 and h_1 are given by (3.11) and (3.12).

Figure 13a shows the upper layer thickness when only the h_0-layer is in motion (as in LPS) in the entire oceanic domain (i.e., no ventilated outcrop at f_v and no eddy-driven motion in the unventilated region.) For this calculation we have chosen

$$\left.\begin{aligned} D_0^2 &= H_0^2\left(1 - \frac{x}{a}\right)\sin\pi\frac{f}{f_0} \\ \frac{H_1}{H_0} &= \frac{1}{2} \\ \frac{\gamma_0}{\gamma_1} &= 1.25 \end{aligned}\right\}.$$

Fig. 13b shows the same upper-layer thickness contours when the first unventilated layer is moving. The only change occurs in the northwest quadrant of the ocean where the upper layer deepens less rapidly to the west than in the previous case. Since the unventilated layer is moving, it carries some of the Sverdrup transport and, therefore, the shear across the first interface is weaker than in the case of only one moving layer and the slope of the interface between them is correspondingly less. The meridional transport in the upper layer is

$$T_0 = h_0 v_0 = \frac{\gamma_0 + \gamma_1}{f} h_0 \frac{\partial h_0}{\partial x}, \quad x < x_1, \quad (3.24)$$

and in the unventilated layer

$$T_1 = h_1 v_1 = \frac{\gamma_1}{f} h_1 \frac{\partial h_0}{\partial x}, \quad x < x_1.$$

Thus

$$\frac{T_0}{T_1} = \left(1 + \frac{\gamma_0}{\gamma_1}\right)\frac{h_0}{h_1}. \quad (3.25)$$

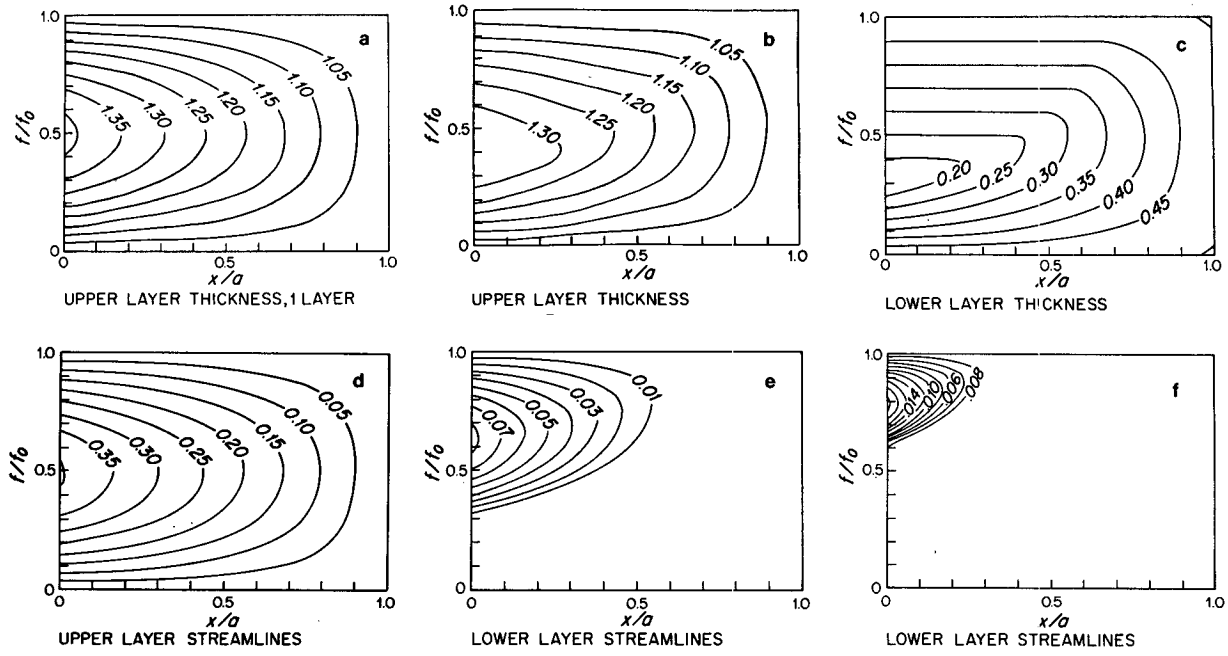

FIG. 13. (a) The thickness of the upper layer when (a) all unventilated layers are motionless and (b) when the uppermost unventilated layer is in motion. (c) The thickness of the uppermost unventilated layer. Its domain of motion is easily seen as the region where its thickness is independent of longitude. (d) The upper-layer [compare with (a)] and (e) the lower-layer streamline pattern. (f) The lower-layer streamline when H_1 is doubled over its value used in (e).

This shows that at $f = f_0$, where $h_n = H_n$, the vertical partitioning of the transport between ventilated and unventilated layers is determined by how one specifies the density field. In particular, if $H_0 = 0$, then all of the transport will be in the unventilated layer. Since h_0 increases southward while h_1 decreases, the tendency is for the transport to shift into the upper ventilated layer as one moves south or west.

Figure 13c shows the lower layer thickness. The region in which the isopleths of h_1 are east–west delineate the constant potential-vorticity pool. With the parameters above, the presence of the pool has a small effect on the meridional transport in the uppermost layer although it has a significant effect on the configuration of the layer depth and hence the isopycnal distribution. Fig. 13d shows the streamline pattern in the upper layer. In the present case, it is hardly distinguishable from the one-moving layer model whose streamlines are coincident with the curves in Fig. 13a. Fig. 13e shows the streamlines in the unventilated layer for the case $H_1 = \frac{1}{2}H_0$. As H_1 or H_0 is increased (see 3.17) the pool of constant potential vorticity is crowded into the northwest corner. Fig. 13f shows the streamline pattern in the case $H_1 = H_0$. Only a small portion of the flow is affected by the pool of constant potential vorticity.

This contrasts considerably with our example of the preceding section. In that case, the basic stratification is limited to the unventilated zone and the pools of homogenized potential vorticity extend all across the basin at depths immediately below the ventilated zone. Those results would obtain here in the limiting case $H_1 \to 0$. (Note that while the ratio H_0/H_1 determines the vertical distribution of the transport, it is the product H_0H_1 that governs the extent of the pool.) It remains unclear to us how to go from the layer model to a continuous model in both ventilated *and* unventilated regions. If both regions are represented, in a gross way, by layers as in this section, the effective lateral extent of the pools becomes limited. Increasing the resolution in only the unventilated region as in Section 2, increases the pool size by allowing shallower zones in eastern regions. We speculate, however, that at the particular latitude where $w_E = 0$, (i.e., at $f = f_0$), the limit $\gamma_n \to 0$, $H_n \to 0$ may recover features of the continuous model. In that case, at *that* latitude, the pool of constant potential vorticity would be gyre-wide. It is not clear how this can be extrapolated to lower latitudes. However, at $f = f_0$, the external forcing is, by definition, zero. Were it to remain weak for $f < f_0$, we know the pools of constant potential vorticity would not extend southward since the isopleths of q would quickly become latitude circles.

Now let us turn our attention to the region south of the outcrop latitude $f = f_v < f_0$ where the layer of thickness h_0 is subducted beneath h_v. There are two separate cases to consider. If the latitude of the density outcrop, $f = f_v$, occurs south of the pool of homogenized potential vorticity defined by $x_1(f)$, then the flow south of $f = f_v$ is identical to that already given in LPS. There are then two moving layers; the subducted layer of

thickness h_0 and the upper warm-water layer of thickness h_v. The more interesting case for our present purpose occurs when the outcrop latitude occurs athwart the pool of constant potential vorticity. In that case both the theory of LPS and the calculation of the flow in the unventilated layer are mutually modified.

As in our earlier discussion for the region north of $f=f_v$, the flow is usefully separated into several domains and these are shown schematically in Fig. 14.

As in LPS, there is a shadow zone between the eastern boundary and the curve $x_v(f)$, labeled 1 in the figure, in which only the upper layer is in motion. The reason for the separation of the subducted layer's flow from the eastern wall is again simply the inability of a fluid column to have constant thickness (to satisfy the zonal flow condition) and conserve potential vorticity while moving along the eastern wall. In this shadow zone [Note that h_v vanishes on $x = a$ as anticipated by (3.8a).]

$$\left.\begin{aligned} h_v &= \left(\frac{\gamma_0}{\gamma_v} D_0^2\right)^{1/2} \\ h_0 &= H_0 - h_v \\ h_1 &= H_1 \end{aligned}\right\}. \tag{3.26}$$

In the region immediately to the west of $x_v(y)$, both the upper layer and the subducted layer are moving and the latter preserves potential vorticity, i.e.,

$$\frac{f}{h_0} = G(h_0 + h_v), \tag{3.27}$$

where G is an arbitrary function of the pressure. The unventilated zone is at rest. Since h_v vanishes at $f = f_v$ it follows, as in LPS, that for all points south of the outcrop

$$G(h_0 + h_v) = \frac{f_v}{h_0 + h_v}$$

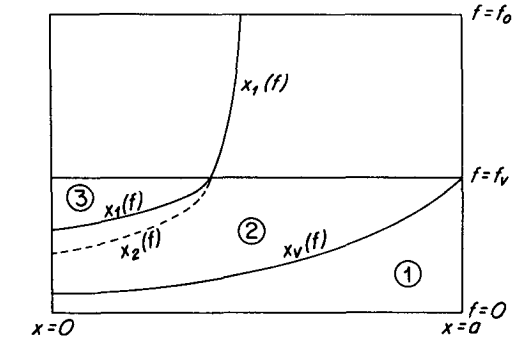

FIG. 14. The domains of flow in plan view when there is one unventilated layer in motion and when the outcrop latitude $f = f_v$ intersects the pool of constant potential vorticity. The critical curves $x_v(f)$, $\tilde{x}_2(f)$ and $x_1(f)$ are described in the text.

so that, as in LPS,

$$\left.\begin{aligned} h_0 &= \frac{f}{f_v}(h_0 + h_v) \\ h_v &= \left(1 - \frac{f}{f_v}\right)(h_0 + h_v) \end{aligned}\right\}, \tag{3.28a, b}$$

while the Sverdrup relation yields

$$h_0 + h_v = \frac{(D_0^2 + H_0^2)^{1/2}}{\left(1 + \frac{\gamma_v}{\gamma_0}(1 - f/f_v)^2\right)^{1/2}}. \tag{3.28c}$$

The separating contour $x_v(f)$ is determined by insisting that h_0 and h_v are continuous along $x_v(f)$, and this yields

$$D_0^2(x_v, y) = \frac{\gamma_v}{\gamma_0} H_0^2\left(1 - \frac{f}{f_v}\right)^2 \tag{3.29}$$

while

$$h_1 = H_0 + H_1 - (h_0 + h_v). \tag{3.30}$$

Aside from a trivial change in notation, the solution in Regions 1 and 2 is identical to those given in LPS.

However, the center of our attention is focused on Region 3. Here three layers are moving. Two are ventilated (one of them having been subducted), while the lowest one is unventilated with constant potential vorticity.

In Region 3,

$$h_1 = \frac{f}{f_0} H_1, \tag{3.31}$$

while the intermediate layer has potential vorticity constant on geostrophic streamlines, i.e.,

$$\frac{f}{h_0} = K[\gamma_1(h_0 + h_1 + h_v) + \gamma_0(h_0 + h_v)]. \tag{3.32}$$

On $f = f_v$, h_v vanishes while h_1 is a constant $(=f_v/f_0 H_1)$. Thus, it is easy to see that

$$K(\theta) = \frac{(\gamma_1 + \gamma_0) f_v}{\theta - \gamma_1 \frac{f_v}{f_0} H_1}, \tag{3.33}$$

where θ is the argument of K. Using (3.32) and (3.33), it follows that

$$h_v = \frac{f_v}{f} h_0\left(1 - \frac{f}{f_v}\right) + \frac{\gamma_1}{\gamma_1 + \gamma_0} H_1 \frac{(f_v - f)}{f_0}. \tag{3.34}$$

When (3.34) and (3.31) are inserted into (3.7) (for $n = 1$), a quadratic for h_0 is obtained which completes the solution in Region 3. The form of the quadratic is sufficiently complicated that little insight is achieved by considering it directly. Perhaps the most important physical result is the effect of adding a new ventilated layer on the extent of the pool of constant potential

vorticity, i.e., what is the continuation of $x_1(f)$ in the region $f < f_v$.

In the region east of $x_1(f)$, the unventilated layer is at rest so that

$$h_1 + h_0 + h_v = H_0 + H_1.$$

That is, the base of the unventilated layer must be at the same level as at the eastern wall. On the other hand, if h_1 is continuous across $x_1(f)$, $h_1 = H_1 f/f_0$. Thus, on $x_1(f)$

$$(h_0 + h_v) = H_0 + H_1(1 - f/f_0) \tag{3.35}$$

which should be compared to (3.16). Evaluating (3.7) on $x_1(f)$ where (3.35) holds yields

$$D_0^2(x_1, y) = 2H_0H_1\left(1 - \frac{f}{f_0}\right) + H_1^2\left(1 - \frac{f}{f_0}\right)^2 + \frac{\gamma_v}{\gamma_0} h_v^2. \tag{3.36}$$

A comparison of (3.36) with (3.10) shows that the effect of adding a new ventilated layer of depth h_v *shrinks* the pool of constant potential vorticity and crowds it farther to the western side of the ocean. We can use (3.34) together with (3.35) to calculate h_v on $x_1(f)$, i.e.,

$$h_v = \left(1 - \frac{f}{f_v}\right)\left\{H_0 + H_1\left[\frac{\gamma_1}{\gamma_0 + \gamma_1}\frac{f}{f_0} + \left(1 - \frac{f}{f_v}\right)\right]\right\},$$

on

$$x_0 = x_1(f), \tag{3.37}$$

and thus determine the boundary of the pool of constant potential vorticity. Fig. 15 shows the result of such a calculation. The parameters are identical to those used in Fig. 13. We have chosen $\gamma_v/\gamma_0 = 1$. The curve marked 0 in the figure is the continuation of (3.17), i.e., the boundary of the pool in the absence of an additional ventilated layer. The curve marked v in the figure shows how the pool shrinks south of the outcrop at $f = f_v$ when a new ventilated layer is added.

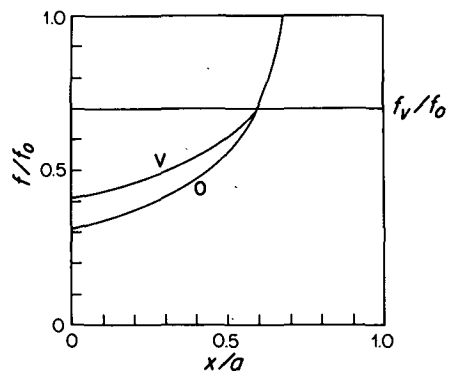

FIG. 15. South of the outcrop latitude $f = f_v$, the pool of constant potential vorticity shrinks in size from the domain bounded by the curve labeled 0 to one bounded by the curve labeled v as a consequence of the addition of another ventilated layer.

The physical reason for the shrinking size of the constant potential-vorticity pool is both simple and important. In the region of the ventilated thermocline, the addition of more layers leads to a fall-off, from layer to layer, of the strength of the wind-driven circulation. As more ventilated layers are added, there is a tendency to trap the motion in the upper warm-water layers. This produces a weaker compression of the stationary unventilated layers and only in the western regions, where D_0^2 (and hence the thickness variations) are greatest, can geostrophic contours distort strongly enough to allow the fluid in those layers to move. The pool of constant potential vorticity is shrunk accordingly. With the parameters chosen above, in the region south of f_v, the Sverdrup transport is carried primarily in the upper ventilated layers. However, there is a change in the isopycnal distribution in the unventilated region due to (3.31).

For the sake of completeness, we need to mention the fact that the solution is not yet formally complete. A buffer region, between the solid and dotted curve in Fig. 14 is required to match the solutions in Regions 2 and 3. In this buffer region between $x_1(f)$ and $\tilde{x}_2(f)$, the unventilated region is at rest, but fluid in the subducted layer which conserves potential vorticity sweeps into this region from the west of the point $x_1(f_v)$ and its K function (3.32) must be altered to reflect this fact. Given the relative smallness of the transport in the unventilated region at these latitudes, the details of the flow are not presented.

4. The subpolar gyre

a. A ventilated model of the subpolar gyre

In the subpolar gyre, as in LPS, we look for a solution in which the unventilated isopycnals rise to the surface. In LPS each layer is motionless until the one above it outcrops (see Fig. 15). What is the continuously stratified analog of this solution? The appropriate generalization of the layered LPS solution is obtained by arguing that in the region where the fluid is in motion the density is uniform vertically. Thus suppose there is a surface $z = -D(x, y)$ below which the fluid is motionless with B given by

$$B = N^2 z \tag{4.1}$$

(see Fig. 16).

Above $z = -D$, the fluid is being removed by Ekman suction at $z = 0$ and so $(u, v, w) \neq (0, 0, 0)$. In this region $B_z = 0$. Continuity of B at $z = -D$ implies

$$B = -N^2 D, \quad \text{if} \quad z > -D, \tag{4.2a}$$

because

$$B = N^2 z, \quad \text{if} \quad z < -D. \tag{4.2b}$$

Now from (2.7)

$$f^2 w_{zz} = -\beta N^2 D_x, \tag{4.3}$$

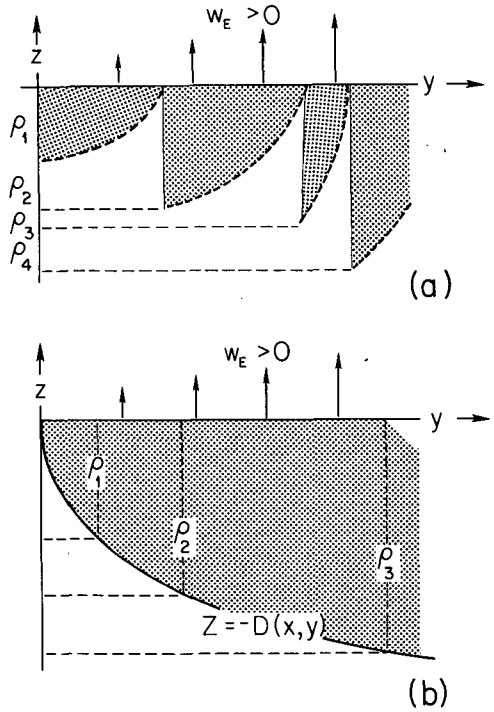

FIG. 16. Schematic meridional density section of the subpolar gyre. (a) Layered stratification—Only the uppermost layer is in motion. All of the Sverdrup transport is confined to the stippled area. (b) Continuous stratification—The dashed lines represent isopycnals. Below $z = -D$, the fluid is motionless. All of the Sverdrup transport is in the stippled region above $z = -D$. As in case (a), only the uppermost density layer is in motion. Case (b) is the limit of case (a) as the number of layers is increased.

and integrating the above with respect to z gives

$$w = -\frac{1}{2}\left(\frac{\beta N^2}{f^2}\right)D_x(z + D)^2, \tag{4.4}$$

where, in analogy with LPS, $w = v = 0$ at $z = -D$. Finally, D is determined by applying the boundary condition at $z = 0$

$$w_E = -\frac{1}{2}(\beta N^2/f^2)D^2D_x \tag{4.5}$$

or integrating to the eastern boundary $x = a$

$$\frac{1}{6}D^3 = \left(\frac{f^2}{\beta N^2}\right)\int_x^a w_E(x', y)dx' \tag{4.6}$$

[compare this with (2.17)].

The subpolar circulation patterns sketched in Figs. 2, 3, 4 and 5 are based on the calculation above.

b. A partially ventilated model of the subpolar gyre

One peculiar feature of the circulation model in the previous subsection is the vertical isopycnals. As an alternative, we now construct a solution in which the ocean is divided into three regions (see Fig. 17):

1) Region I where $0 > z > -D(x, y)$ and $B_z = 0$,
2) Region II where $-D(x, y) > z > -G(x, y)$ and $q = fB_z = f_0N^2$,
3) Region III where $-G(x, y) > z > -\infty$ and $B = N^2z$ as in (3.1) while $(u, v, w) = (0, 0, 0)$.

The dynamics of Region I are similar to those of the subpolar gyre in Section 3. Region II on the other hand has uniform potential vorticity.

Begin by observing that in Region II

$$B = \left(N^2\frac{f_0z}{f}\right) + b(x, y), \quad \text{if} \quad -G < z < -D. \tag{4.7}$$

Continuity of B at $z = -G$ gives

$$B = \left(N^2\frac{f_0}{f}\right)\left[z - \left(1 - \frac{f_0}{f}\right)G\right], \quad \text{if} \quad -G < z < -D. \tag{4.8}$$

Continuity of B at $z = -D$ gives B everywhere in Region I

$$B = -\left(N^2\frac{f_0}{f}\right)\left[D + \left(1 - \frac{f_0}{f}\right)G\right], \quad \text{if} \quad -D < z < 0. \tag{4.9}$$

One can now calculate w from (2.7). As in the previous examples one integrates upwards, starting at $z = -G$ where

$$w = w_z = 0.$$

Thus in Region II

$$w = -\frac{1}{2}\left(\frac{\beta N^2}{f^2}\right)\left(\frac{f - f_0}{f}\right)(z + G)^2G_x, \tag{4.10a}$$

$$v = -\left(\frac{N^2}{f}\right)\left(\frac{f - f_0}{f}\right)(z + G)G_x. \tag{4.10b}$$

In Region I we again obtain v and w from (2.5) and (4.12). Since the density is continuous, v and w are continuous at $z = -D$. One finds

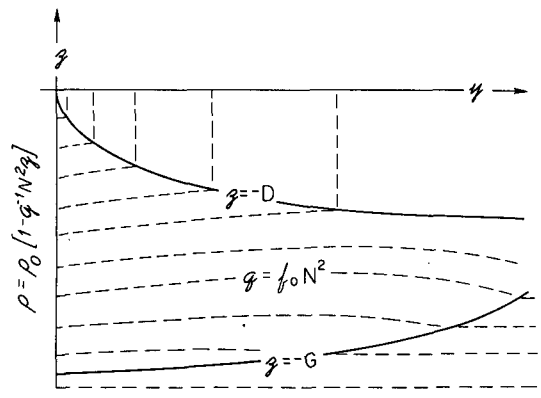

FIG. 17. Schematic meridional density section of the subpolar gyre. The dashed curves represent isopycnals. Above $z = -D$, the isopycnals are vertical. Between $z = -D$ and $z = -G$, the potential vorticity is uniform. Below $z = -G$, the fluid is motionless.

$$w = -\frac{1}{2}\left(\frac{\beta N^2}{f^2}\right)\left(\frac{f-f_0}{f}\right)(z+G)^2 G_x - \frac{1}{2}\left(\frac{\beta N^2}{f^2}\right)\left(\frac{f_0}{f}\right)(z+D)^2 D_x, \quad (4.11)$$

if $0 > z > -D(x, y)$.

Finally since $w = w_E$ at $z = 0$ one has

$$w_E = -\frac{1}{2}\left(\frac{\beta N^2}{f^2}\right)\left[\left(\frac{f-f_0}{f}\right)G^2 G_x + \left(\frac{f_0}{f}\right)D^2 D_x\right]. \quad (4.12)$$

This equation is only one relation between the two unknowns G and D. Thus there are an infinite number of solutions since one is free to specify an additional arbitrary relationship between G and D.

One choice is $G = D$, in which case (4.12) reduces to (4.6). In this case there is no Region II and the isopycnals are vertical in the subpolar gyre. This is just the model from the previous subsection.

An alternative (and more plausible) choice is $D = 0$. In this case there are no vertical isopycnals and the potential vorticity is uniform everywhere in the subpolar gyre. This is essentially the solution given by RY.

This particular set of solutions illustrates one of the principal conclusions of this article: there are an infinite number of solutions of the planetary geostrophic equations all of which satisfy the same boundary conditions. Other physical processes, not explicit in the equations themselves, must be invoked to pick a solution. For example, *a priori* it seems unlikely that isopycnals are vertical in the subpolar gyre so $D = 0$ in (4.15). On the other hand, one might argue that there is very strong thermally driven vertical mixing in the subppolar gyre which vertically homogenizes the density field to some depth D. One could probably construct a simple model in which D is determined by the heat flux from the ocean to the atmosphere. This interesting possibility reinforces the original conclusion: additional physics is required to obtain a unique solution.

The subpolar circulation patterns sketched in Figs. 7, 8, 9 and 10 are obtained from the calculation above. In these figures we have taken $D = 0$, so there are no vertical isopycnals.

5. Conclusions

We have presented a model in which the ventilated thermocline theory of LPS is linked with the theory of potential vorticity homogenization of RY. There are several important conclusions we wish to emphasize.

First, although the regions of ventilation and homogenization are spatially distinct, they interact and affect one another non-linearly since the regions must combine to carry the Sverdrup transport. Second, the partition of the transport between the ventilated and unventilated regions depends on the gross stratification in each region. In Section 2, where the ventilated zone consists of a single homogeneous layer bounded below by a uniformly stratified zone, the transport in the unventilated region is a rather large proportion of the total and the pool of constant potential vorticity occupies a large extent of the subtropical gyre. The layered model of Section 3 shows how the presence of ventilated outcrop layers can shrink the size of the pools of constant potential vorticity in the unventilated layers. The addition of these extra ventilated layers in the northern part of the subtropical gyre (where $\partial D_0^2/\partial y < 0$) raises the possibility that, as in LPS, new pools of constant potential vorticity will appear up against the western boundary within the ventilated layers.

We have also argued that the layered model of Section 3 may be a good representation of the continuous model as the layer thickness goes to zero at $f = f_0$ where w_E vanishes. Then, at least at $f = f_0$ the constant potential vorticity pool must extend across the basin without regard to the stratification in the ventilated zone. However, its southward extent in the general case is uncertain.

In both models, the pools of constant potential vorticity are basin-shaped, deepen to the northwest, and are similar in structure to the pools found in the quasi-geostrophic, β-plane models of RY.

Third, we wish to emphasize that the ventilated thermocline model without potential vorticity homogenization is most likely at least locally unstable. The condition that the potential vorticity isopleths of the unventilated layers significantly depart from latitude circles deformed by the β-effect is qualitatively similar to the usual necessary conditions for quasi-geostrophic instability on the mesoscale. In these regions where we have hypothesized the result will be homogenization of potential vorticity, the geography of the density surfaces of the unventilated regions will be affected. As we have remarked above, this may or may not significantly affect the transport in the ventilated region.

Finally, we would again like to stress the hypothetical nature of our solution for the flow in the unventilated zone. Our hypothesis of potential vorticity homogenization depends implicitly on the nature of mesoscale potential vorticity mixing and on the interaction of the mid-ocean gyre with the western boundary current regions (see especially Ierley and Young, 1983). These are all uncertain elements in our theory. This study emphasizes the importance of dissipation in selecting a unique solution. It is ironic that after twenty years of contriving similarity "solutions" which are unable to satisfy both horizontal and vertical boundary conditions, it is now a simple matter to construct a variety of solutions all of which satisfy the same physically reasonable boundary conditions.

We would prefer to consider models that have completely continuous distributions of density and velocity in all regions of the flow. So far that goal has eluded

us and we have been forced, especially in the ventilated region, to represent the solution in terms of finite layers of uniform density. The exact relation of these models to a continuous model is still obscure. In these layered models the structure of the wind-driven flow is sensitive to the initial specification of the density field [e.g., in determining the size of the constant potential-vorticity pool, the effects of decreasing H_0, H_1 and γ_0 in (3.20) are multiplicative]. Clearly more observational or theoretical guidance than the present study has brought to bear on this issue is required.

Acknowledgments. WRY is supported by the Office of Naval Research Grant N00014-79-C-0472. JP is supported by a grant from the National Science Foundation's Division of Atmospheric Sciences.

REFERENCES

Gill, A. E., 1982: *Atmosphere–Ocean Dynamics.* Academic Press, 662 pp.

Holland, W. R., 1983: Regions of uniform potential vorticity in circulation models with mesoscale resolution. In preparation.

Ierley, G. R., and W. R. Young, 1983: Can the western boundary layer affect the potential vorticity distribution in the Sverdrup interior of a wind gyre? *J. Phys. Oceanogr.*, **13**, 1753–1763.

Luyten, J. L., J. Pedlosky and H. Stommel, 1983: The ventilated thermocline. *J. Phys. Oceanogr.*, **13**, 292–309.

Montgomery, R. B., 1938: Circulation in upper layers of southern North Atlantic deduced with use of isentropic analysis. *Pap. Phys. Oceanogr. Meteor.*, **6**, 55 pp.

Needler, G., 1967: A model for the thermohaline circulation in an ocean of finite depth. *J. Mar. Res.*, **25**, 329–342.

Pedlosky, J., 1979: *Geophysical Fluid Dynamics,* Springer-Verlag, 624 pp.

Phillips, N. A., 1963: Geostrophic motion. *Rev. Geophys.*, **1**, 123–176.

Rhines, P. B., and W. R. Holland, 1979: A theoretical discussion of eddy driven mean flows. *Dyn. Atmos. Oceans,* **3**, 289–325.

——, and W. R. Young, 1982a: A theory of the wind-driven circulation I. Mid-Ocean Gyres. *J. Mar. Res.*, **40**(Suppl.), 559–596.

——, and ——, 1982b: Homogenization of potential vorticity in planetary gyres. *J. Fluid Mech.*, **122**, 347–367.

Welander, P., 1971: Some exact solutions to the equations describing an ideal fluid thermocline. *J. Mar. Res.*, **29**, 60–68.

Young, W. R., and P. B. Rhines, 1982: A theory of the wind-driven circulation II. Circulation models and western boundary layer. *J. Mar. Res.*, **40**, 849–872.